Parallel 3-D Aerodynamic Shape Optimization on Unstructured Meshes

Sang Wook Lee* and Oh Joon Kwon**
Department of Aerospace Engineering
Korea Advanced Institute of Science and Technology, Daejeon, Korea 305-701

Abstract

A three-dimensional aerodynamic shape optimization technique in inviscid compressible flows is developed by using a parallel continuous adjoint formulation on unstructured meshes. A new surface mesh modification method is proposed to overcome difficulties related to patch-level remeshing for unstructured meshes, and the effect of design sections on aerodynamic shape optimization is examined. Applications are made to three-dimensional wave drag minimization problems including an ONERA M6 wing and the EGLIN wing-pylon-store configuration. The results show that the present method is robust and highly efficient for the shape optimization of aerodynamic configurations, independent of the number of design variables used.

Key Word : Continuous Adjoint Method, Shape Optimization, Unstructured Meshes, Parallel Computation, Tightly Coupled Optimization Algorithm

Introduction

Currently, Computational Fluid Dynamics techniques are widely used not only to simulate and understand the complicated flow physics, but also to design optimum aerodynamic shape of air vehicles which provides maximum performance at the desired operating condition. Recently, various aerodynamic shape optimization techniques have been investigated along with the rapid development of efficient numerical algorithms. One of the most popular methods currently available is the gradient-based optimization technique in which a specified objective function is to be minimized. The gradient of the objective function with respect to the design variables, which is called sensitivity, is used to update the design variables in the direction where value of the objective function can be reduced in a systematic way.

Several researches have been previously made for the evaluation of the sensitivity for aerodynamic applications. Recently, a particular interest is given to adjoint method, in which sensitivities are found without calculating the variation of the flow variables. Thus, this method has an advantage of requiring less memory and computational time compared to the discrete adjoint method or any other sensitivity analysis methods.

Continuous adjoint method was initially developed by Jameson for both potential and Euler equations[1]. Further extension was made for two- and three-dimensional applications on multi-block structured grids with viscous effect[2]. Continuous adjoint method on unstructured meshes was first introduced by Anderson and Vankatakrishnan for two-dimensional aerodynamic shape optimization[3]. Recently, sensitivity formulation of the general cost function was developed by Baysal[4]. Boundary condition and affordable objective function for

* Graduate Research Assistant
** Associate Professor
E-Mail : ojkwon@mail.kaist.ac.kr, TEL : 042-869-3720, FAX : 042-869-3710

unstructured meshes were also developed by Arian[5]. However, continuous adjoint method on unstructured meshes are mostly limited to applications to simple two-dimensional flow problems.

In the present study, a technique for the aerodynamic sensitivity analysis and the shape optimization for three-dimensional configurations are developed in inviscid compressible flow by using a continuous adjoint method on unstructured meshes. In order to achieve realistic shape optimization, sensitivity analysis based on a fully linearized adjoint flux is adopted. For robust geometry handling, a new surface mesh modification technique is also developed for the interpolation of the design variables. The efficiency of the optimization is enhanced by using a tightly-coupled design algorithm in conjunction with parallelization. Applications are made for drag minimization of a transonic ONERA M6 wing and the EGLIN wing-store-pylon configuration.

Numerical Method

Governing Equations

The governing Euler equations can be written in an integral form over a control volume V:

$$\frac{\partial}{\partial t}\int_V \boldsymbol{Q}dV+\oint_S \boldsymbol{F}(\boldsymbol{Q},\boldsymbol{n})dS=0 \tag{1}$$

The inviscid flux, $\boldsymbol{F}(\boldsymbol{Q},\boldsymbol{n})$, across each cell face is discretized based on the Roe's flux-difference splitting formula. The second-order spatial accuracy is obtained by using the Laplacian averaging reconstruction method[6]. An implicit time integration algorithm based on the linearized Euler backward-differencing is used to derive the solution to steady state. Local time stepping is applied to accelerate the convergence of the solution. The resulting linear system of equations is solved at each iteration by using a point Gauss-Seidel method.

Adjoint Equations

The objective function for aerodynamic shape optimization is expressed as an integral form about the pressure over the surface :

$$I_c=\int_B g(\boldsymbol{Q}(\boldsymbol{D}))\cdot k(\boldsymbol{D})ds \tag{2}$$

where $g(\boldsymbol{Q}(\boldsymbol{D}))$ and $k(\boldsymbol{D})$ are the functions of flow variables and geometry, respectively. To transform the constraint optimization problem into an unconstraint optimization problem, the Lagrangian multiplier, which is known as the adjoint variable, is introduced. Then the new cost function is defined as:

$$\begin{aligned} I(\boldsymbol{Q},\boldsymbol{D},\boldsymbol{\Psi}) &= I_c(\boldsymbol{Q},\boldsymbol{D})+\int_\Omega(\boldsymbol{\Psi},\boldsymbol{R})\,d\Omega \\ &= I_c(\boldsymbol{Q},\boldsymbol{D})+I_R(\boldsymbol{R},\boldsymbol{\Psi}) \end{aligned} \tag{3}$$

where $\boldsymbol{\Psi}$ is the vector of the adjoint variables (Lagrangian multipliers), $\boldsymbol{D}$ is the vector of the design variables, and $\boldsymbol{R}$ represents the steady-state flow equations.

$$\boldsymbol{R}=\frac{\partial \boldsymbol{F}}{\partial x}+\frac{\partial \boldsymbol{G}}{\partial y}+\frac{\partial \boldsymbol{H}}{\partial z}=0 \tag{4}$$

The adjoint equations of the three-dimensional Euler equations are obtained by taking the variation of equation (3) and regrouping terms:

$$\frac{\partial \boldsymbol{\Psi}}{\partial t}-A^T\frac{\partial \boldsymbol{\Psi}}{\partial x}-B^T\frac{\partial \boldsymbol{\Psi}}{\partial y}-C^T\frac{\partial \boldsymbol{\Psi}}{\partial z}=0 \tag{5}$$

where A, B, and C are the flux jacobian matrices. The boundary condition can also be obtained as:

$$k_x\Psi_2 + k_y\Psi_3 + k_z\Psi_4 + k\frac{\partial g(p)}{\partial p} = 0 \tag{6}$$

where p is the pressure and k_x, k_y, k_z are the face normal vectors. Then the adjoint sensitivity can be expressed as :

$$\delta I = \int_B R(\Psi_1 + u\Psi_2 + v\Psi_3 + w\Psi_4 + H_t\Psi_5)ds + \int_B \tilde{k}(\boldsymbol{D})g(\boldsymbol{Q})ds \tag{7}$$

where

$$\begin{aligned} R = & -\hat{x}\left(\frac{\partial Q_2}{\partial x}k_x + \frac{\partial Q_3}{\partial x}k_{y+}\frac{\partial Q_4}{\partial x}k_z\right) - \hat{y}\left(\frac{\partial Q_2}{\partial y}k_x + \frac{\partial Q_3}{\partial y}k_y + \frac{\partial Q_4}{\partial y}k_z\right) \\ & -\hat{z}\left(\frac{\partial Q_2}{\partial z}k_x + \frac{\partial Q_3}{\partial z}k_y + \frac{\partial Q_4}{\partial z}k_z\right) - (Q_2\tilde{k}_x + Q_3\tilde{k}_y + Q_4\tilde{k}_z) \end{aligned} \tag{8}$$

The linear adjoint equations can be discretized by using an any stable and consistent method. However, in order to obtain accurate sensitivity, the adjoint discretization method must be consistent with that of the flow equations[7]. In the present study, the discrete adjoint residual is initially derived from the discrete adjoint formulation, and then the continuous adjoint flux is obtained from the guidance of discrete adjoint residual[7]. The resulting adjoint flux can be written as :

$$G_{i,j} = \frac{1}{2}\left(A_i^T(\Psi_L + \Psi_R) + \left(\frac{\partial \Phi}{\partial \boldsymbol{Q}}\right)^T(\Psi_R - \Psi_L)\right) \tag{9}$$

where $\Phi = |\tilde{A}|(\boldsymbol{Q}_R - \boldsymbol{Q}_L)$. Typically, two forms of the adjoint flux are available depending on the linearization of Φ. One is the fully linearized adjoint flux including the derivation of the Roe-averaged matrix, and the other is the approximately linearized adjoint flux obtained by assuming that the Roe-averaged matrix is constant. In the present study, both methods are used to examine the accuracy of the solution. Derivation of the Roe-averaged matrix is made numerically to reduce computational time[8].

Since the mathematical characteristics of the adjoint equations is hyperbolic, same as that of the Euler equations, many of the subroutines developed for the flow solver, can be used for the analysis of the adjoint equations with little modification. Since, the derivation of the flux jacobian matrix which is essential for the discrete adjont method, is not required, continuous adjoint method is more efficient in time and memory.

Shape Function and Mesh Movement

During the aerodynamic shape optimization process, deformation of the surface geometry must be reflected in the field cells. In the present study, Hicks-Henne functions are used as the shape function, and the mesh movement is adjusted by using the spring analogy.

It is well known that selection of design variables significantly affects the designed result. Too many design variables may create undesirable numerical noise and result in poor computational efficiency, while insufficient number of design variables causes poor result[1]. Thus, selection of proper design variables is a very important issue.

In three-dimensional shape optimizations,

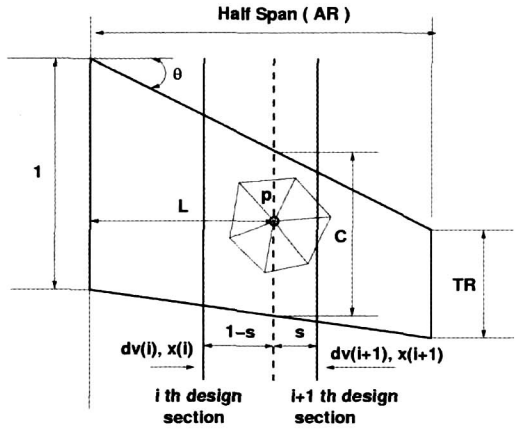

Fig. 1. Schematic view of interpolation of design variables.

design variables are usually defined at selected design sections. During the design process, airfoil shapes at the sections are modified by using the shape function, and the remaining surface geometry is modified through proper interpolation. However, the mesh points are usually not aligned along the specified design sections for unstructured meshes. To overcome this difficulty, a new interpolation method is introduced such that the value of design variables at the specified design sections can be obtained from the surrounding surface node points though linear interpolation as in figure 1[9]. Design variables at an arbitrarily located point p between $(i)-th$ and $(i+1)-th$ design sections are computed by using the following formula:

$$dv=(1-s)\times dv(i)+s\times dv(i+1) \tag{10}$$

where s represents the distance from p to $(i+1)-th$ design section.

Optimization Algorithm

In second-order optimization algorithms such as BFGS or FR, Hessian matrix is approximated by one-dimensional search. Thus, selection of the one-dimensional search can significantly affect the designed results[10]. However, accurate one-dimensional search requires fully converged flow solutions. Thus, this costly search procedure becomes one of the main obstacles of the optimization process, particularly in three-dimensions, making the sequential design algorithm not suitable. In the present study, a tightly coupled design algorithm is used[11], in which the time consuming one-dimensional search is replaced by a simple function:

$$\varepsilon=-\frac{G^T\nabla_d GS}{S^T(\nabla_d G)^T\nabla_D GS} \tag{11}$$

where, G represents the gradient, S is the search direction, and $\nabla_d G$ is the Hessian matrix. The Hessian matrix is evaluated by taking the finite-difference of the gradient. This tightly coupled design algorithm does not require fully converged adjoint or flow solutions in the sensitivity analysis, and is very efficient compared to the sequential design algorithm.

Parallel Implementation

In order to handle large scale problems more efficiently, the present design code is parallelized. Domain decomposition is made by partitioning the global computational domain into local sub-domains using the MeTiS library[12]. Message Passing Interface (MPI) is used for the communication of flow variables through communication boundaries.

This parallelization involves separate treatment of each design procedure such as flow solver, adjoint solver, mesh perturbation, and gradient integration. No attempt is made to parallelize the optimization algorithm because this portion is computationally negligible compared to the other elements of the design process. All calculations were made on a PC-based linux cluster having 1.7GHz CPUs.

Results and Discussion

Sensitivity Analysis

As previously mentioned, careful discretization is required to obtain gradients, which are consistent with those obtained by the finite-difference approach. Figure 2 shows the comparison of the gradients obtained by using the adjoint and finite-difference

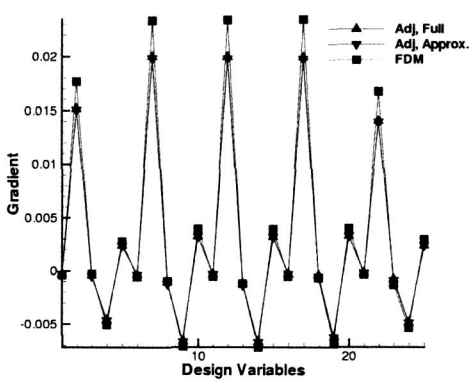

Fig. 2. Comparison of adjoint and finite-difference gradients.

methods for the drag minimization of a three-dimensional infinite NACA0012 wing. Comparison is also made between sensitivities with full and approximately linearized flux Jacobians. The flight condition is at the freestream Mach number of 0.75 and the angle-of-attcack of 1.747 degrees. Good agreement is obtained between the present adjoint method and the one from the finite-difference method. The difference between the full and approximate linearization of the Roe-averaged matrix is not very significant, even though the full linearization is usually known to provide consistently more accurate sensitivity. The computational overhead for the linearization of the Roe-averaged matrix is less than 10% of the total CPU time.

Design Examples

As an initial validation, an ONERA M6 wing is chosen for drag minimization at the flight condition of $M_\infty = 0.83$ and $\alpha = 3.06^o$. Figure 3 shows the surface mesh of ONERA M6 wing. Computational domain is divided into 8 sub-domains by using the MeTiS library, and the bold lines in the figure represent the communication boundaries.

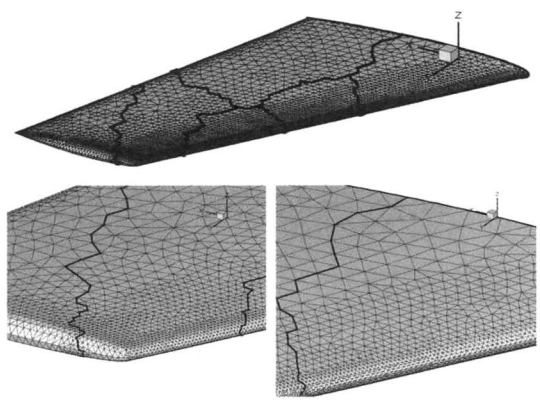

Fig. 3. Surface meshes of the ONERA M6 wing.

Along the design process, the wave drag is to be minimized by removing strong shock waves existing on the upper surface of the wing, while maintaining the desired lift. The objective

Table 1. Location of design sections.

case	# of Design Section	Location of design section (semi span)	obj/obj0
1	2	0, 100 %	0.6955
2	5	0, 25, 50, 75, 100 %	0.5975
3	5	0, 55, 70, 85, 100%	0.5895
4	10	0, 11, 22, ···, 88, 100 %	0.6144
5	21	0, 5, 10, 15, ···, 95, 100%	0.5828
6	31	0, 3.3, 6.7, 10, ···, 93.3, 96.7, 100%	0.5816

function for this problem can be written as:

$$I = \frac{1}{2}(C_L - C_{L,0})^2 + \frac{10}{2} C_D^2 \tag{12}$$

where $C_{L,0}$ is the initial or desired lift coefficient.

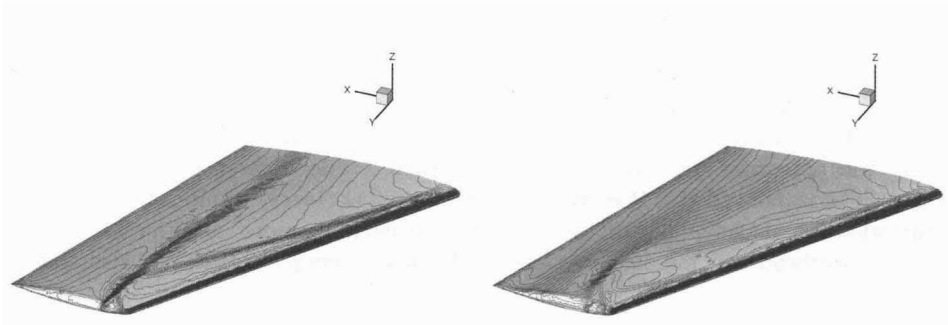

ONERA M6 wing. Designed wing.

Fig. 4. Comparison of surface pressure distributions.

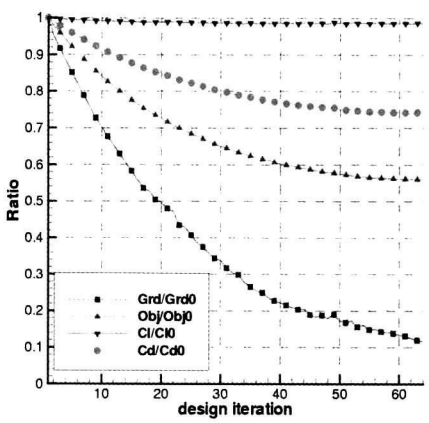

Fig. 5. Convergence history of the ONERA M6 wing.

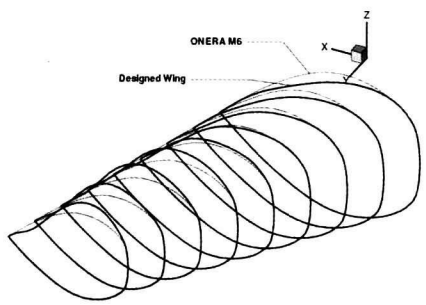

Fig. 6. Surface shape of the ONERA M6 and designed wings.

Six cases were tested to examine the effect of design sections selected arbitrarily as shown in table 1. It was found that different choice of the design sections can significantly affect to the designed results. Since the design variables can be considered as the 'gradient observer' at each design section, insufficient design variables can cause incorrect observation of the gradient and may produce poorly designed results as for case 1. As the number of design variables increases, detail observation of the gradient becomes possible, and better design result is obtained. However, this is not always true as shown for cases 4~6, and there exists possibility of numerical noise in the sensitivity and the existence of local minimum for over-defined design variables[1]. Case 2 and 3 demonstrate the importance of selecting the location of design sections. It is shown that case 3 exhibits better design than that of case 2 for same number of design sections.

Surface pressure contours on the original ONERA M6 and the designed wings are compared in figure 4. It is shown that the strong lambda-shaped shock wave on the upper surface of the original wing mostly disappeared after shape optimization. The drag is reduced to 74% of that of the original wing. However, the change in lift is maintained less than 2% of the initial value as shown in figure 5. Figure 6 shows comparison of surface contours of the ONERA M6 and designed wings. The root section of the designed wing is thinner than that of the ONERA M6 wing, while the tip section becomes thicker than that of the original wing. This is due to the lack of geometric constraints, which are very difficult to implement and require more intensive research.

The second application was made for the EGLIN wing-pylon-store configuration at a free stream Mach number of 0.95 and the angle-of-attach of one degree. The computational mesh consists of 478,370 tetrahedral cells and 90,145 nodes. Figure 7 shows the surface mesh on the

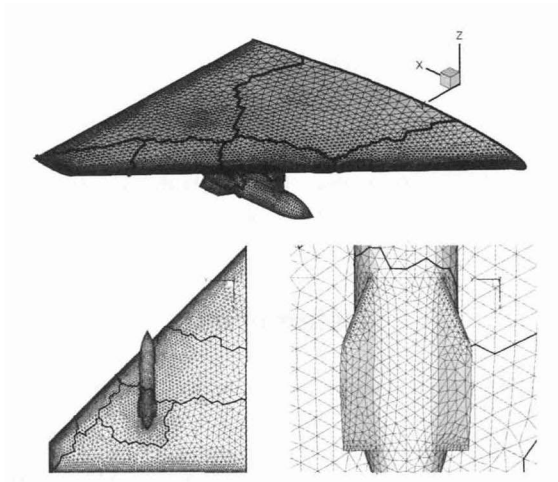

Fig. 7. Surface meshes of EGLIN configuration.

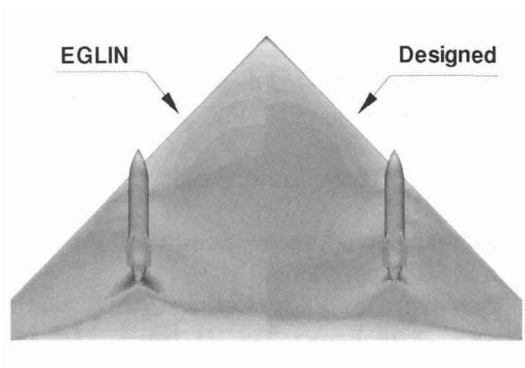

Fig. 8. Comparison of the surface pressure distributions.

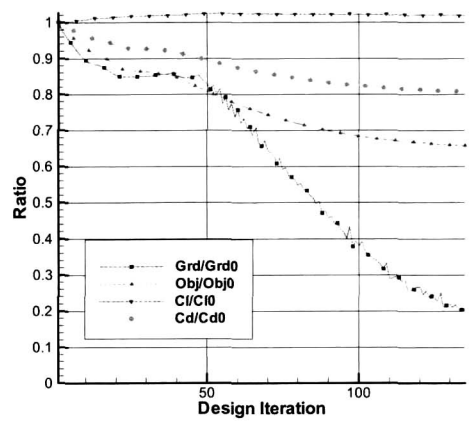

Fig. 9. Convergence history of the EGLIN configuration.

EGLIN configuration. The computational domain was divided into eight sub-domains as represented by the bold lines in the figure. Five design variables were used for each of the five design sections (10, 30, 50, 70, 90% of the semi span) on the lower surface to remove the strong shock wave evident at the rear portion of the pylon. Once the shape optimization was completed, it is observed that the strong shock wave is mostly removed as shown in figure 8. The calculation was made with design variables defined only on the wing surface. Thus, complete elimination of the shock wave is not currently possible without concurrent shape optimization of the pylon configuration. However the pressure drag was reduced by 20% with a slight increase of the lift after 134 iterations as shown in figure 9.

Conclusions

In the present study, a parallel aerodynamic shape optimization method has been developed by using a continuous adjoint formulation on unstructured meshes. Calculation of accurate gradients is achieved by obtaining the continuous adjoint flux from the guidance of the discrete adjoint residual. A mesh independent surface deformation technique is developed to

interpolate the design variables at arbitrarily selected design sections under the unstructured mesh environment. A tightly coupled design algorithm is used for the enhancement of design efficiency.

The present method has been tested to ONERA M6 wing shape optimization using various design sections. Importance of selecting design sections was demonstrated for computational efficiency and designed results. The method has also been applied to the EGLIN wing-pylon-store configuration. It was shown that the present method is an efficient tool for the shape optimization of complex three-dimensional realistic configurations.

References

1. Jameson, A., "Aerodynamic Design via Control Theory," J. of Scientific Computing, Vol. 3, 1988, pp. 233-260.

2. Sangho Kim, Alonso, J. J., and Jameson, A., "Design Optimization of High-Lift Configurations Using a Viscous Continuous Adjoint Method," AIAA-2002-0844, 2002.

3. Anderson, W. K. and Venkatakrishnan, V., "Aerodynamic Design Optimization in Unstructured Grids With a Continuous Adjoint Formulation," AIAA-97-0643, 1997.

4. Baysal, o. and Ghayour, K., "Continuous Adjoint Sensitivities for Optimization With General Cost Functions on Unstructured Meshes," AIAA Journal, Vol. 39, No. 1, 2001, pp. 48-55.

5. Arian, E. and Salas, M. D., "Admitting the Inadmissible : Adjoint Formulation for Incomplete Cost Functions in Aerodynamic Optimization,"AIAA Journal, Vol. 37, No. 1, 1999, pp. 37-44.

6. Frink, N. T., "Rescent Progress Toward a Three-Dimensional Unstructured Navier-Stokes Flow Solver," AIAA-94-0061, 1994.

7. Chun-ho Sung and Jang Hyuk Kwon, "Accurate Aerodynamic Sensitivity Analysis Using Adjoint Equations," AIAA Journal, Vol. 32, No. 2, 2000, pp. 243-250.

8. Sang Wook Lee and Oh Joon Kwon, "Aerodynamic Shape Optimization Using a Continuous Adjoint Formulation on Unstructured Meshes," J. of KSAS, Vol. 30, No. 4, 2002, pp. 18-27.

9. Sang Wook Lee and Oh Joon Kwon, "Aerodynamic Shape Optimization by Using a Continuous Adjoint Method on Unstructured Meshes," Proceeding of JSASS 16th International Sessions in 40th Aircraft Symposium, Yokohama, Japan, 2002, pp. 95-98.

10. Belegundu, A. D. and Chandruoatla, T. R., "Optimization Concepts and Applications in Engineering," ISBN 0-13-031279-7, 1999.

11. Chun-ho, Sung and Jang Hyuk Kwon, "Efficient Aerodynamic Design Method Using a Tightly Coupled Algorithm," AIAA Journal, Vol. 40, No. 9, 2002, pp. 1839-1845.

12. Karypis, G. and Kumar, V., "Multilevel k-way Partitioning Scheme for Irregular Graphs," J. of Parallel and Distributed Computing, Vol. 48, No. 1, 1998, pp. 96-129.